

Performance of cavity-parametric amplifiers, employing Kerr nonlinearites, in the presence of two-photon loss

Bernard Yurke

Bell Laboratories, Lucent Technologies, 600 Mountain Avenue, Murray Hill, NJ 07974

Eyal Buks

Microelectronics Research Center, Technion, Haifa 32000 Israel

(Dated: December 2, 2024)

Two-photon loss mechanisms often accompany a Kerr nonlinearity. The kinetic inductance exhibited by superconducting transmission lines provides an example of a Kerr-like nonlinearity that is accompanied by a nonlinear resistance of the two-photon absorptive type. Such nonlinear dissipation can degrade the performance of amplifiers and mixers employing a Kerr-like nonlinearity as the gain or mixing medium. As an aid for parametric amplifier design, we provide a quantum analysis of a cavity parametric amplifier employing a Kerr nonlinearity that is accompanied by a two-photon absorptive loss. Because of their usefulness in diagnostics, we obtain expressions for the pump amplitude within the cavity, the reflection coefficient for the pump amplitude reflected off of the cavity, the parametric gain, and the intermodulation gain. Expressions by which of the degree of squeezing can be computed are also presented.

PACS numbers: 42.50.Gy, 42.65.Yj, 42.50.Dv

I. INTRODUCTION

Sensitive superconducting microwave devices such as SIS mixers [1, 2] and parametric amplifiers [3, 4] have been devised which achieve performances close to the quantum limit. Phase-sensitive Josephson-junction parametric amplifiers have been constructed whose noise performance exceeds that of the quantum limits imposed on linear phase-insensitive parametric amplifiers [5]. These phase-sensitive amplifiers have been used to generate quantum mechanical states of the electromagnetic field, called squeezed states, whose noise in one amplitude component is reduced below that of vacuum fluctuations. The kinetic inductance of superconducting transmission lines could also be used to make low-noise parametric amplifiers. However, associated with the kinetic inductance is a nonlinear resistance that can degrade device performance. These nonlinear effects are relatively strong in superconducting striplines and microstrips due to the nonuniform distribution of the microwave current along the cross section of the transmission line. Along the edges, where the current density obtains its peak value, the current density can become overcritical even with relatively moderate power levels. As a result, the superconducting current density may vary and, consequently, both inductance and resistance per unit length become current dependent [6]. The kinetic inductance provides a Kerr-like nonlinearity suitable for the construction of parametric amplifiers which employ four-wave mixing. The nonlinear resistance, to lowest order, is of the two-photon absorptive type. To aid in the design of parametric microwave amplifiers which employ kinetic inductance we have preformed an analysis of cavity parametric amplifiers employing a Kerr nonlinear element for gain and a two-photon absorptive loss. Although the analysis was carried out with a specific application in mind [7], it is

more generally applicable, since two-photon absorptive processes often accompany Kerr nonlinearities. There are optical [8, 9, 10] and mechanical [11] systems with such combinations of nonlinearities.

Squeezing in a parametric amplifier with a two-photon absorber has been studied by a number of workers [10, 12, 13, 14]. In the analysis provided here, we present expressions for the amplitude of the pump field within the cavity, the reflection coefficient for the pump off the cavity, the intermodulation gain, and the degree of squeezing. The first, second, and third of these quantities are particularly useful for extracting model parameters from experimental data. The equations of motion are derived using the input-output theory of Gardiner and Collett [15, 16]. The undepleted pump approximation is then made, allowing the pump field inside the cavity and the pump field reflected from the cavity to be calculated. The small signal response is then obtained by linearization about the pump field.

II. THE HAMILTONIAN

The theoretical model of a cavity parametric amplifier possessing a Kerr nonlinearity and a two-photon absorber is seen schematically in Fig. 1. The a_1 port serves as the input-output port. Operated as an amplifier, the signal returned or "reflected" from the input port is larger than the incoming signal. This mode of operation, at microwave frequencies, is referred to as the negative-resistance reflection mode. Port a_2 serves as a linear loss port. Port a_3 serves as the two-photon loss port. The coupling of the a_3 loss mode to the resonator mode A is nonlinear and given in Eq. (9).

It is convenient to write the Hamiltonian as a sum of

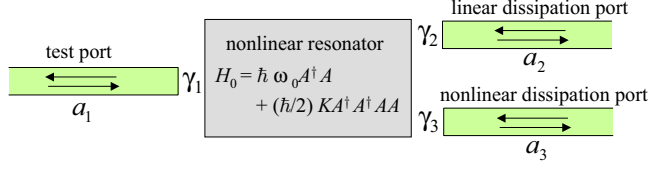


FIG. 1: The model includes nonlinear resonator coupled to three ports, a test port, a linear dissipation port and a nonlinear one.

eight terms,

$$H = H_A + H_K + H_{a_1} + H_{a_2} + H_{a_3} + H_{T_1} + H_{T_2} + H_{T_3}, \quad (1)$$

each representing the Hamiltonian for a component of the system. The Hamiltonian H_A for the cavity mode employed in parametric amplification is given by

$$H_A = \hbar\omega_0 A^\dagger A. \quad (2)$$

The Hamiltonian H_K for the Kerr nonlinearity is given by [17, 18]

$$H_K = \frac{\hbar}{2} K A^\dagger A^\dagger A A. \quad (3)$$

As illustrated in Fig. 1, the cavity is taken to be in contact with three baths. One bath models the external modes that couple to the resonator mode through the port that serves both as the input port and as the output port. The Hamiltonian H_{a1} for this bath is given by

$$H_{a1} = \int d\omega \hbar\omega a_1^\dagger(\omega) a_1(\omega). \quad (4)$$

The other two baths are associated with the linear and nonlinear cavity losses and their Hamiltonians are given by

$$H_{a2} = \int d\omega \hbar\omega a_2^\dagger(\omega) a_2(\omega) \quad (5)$$

and

$$H_{a3} = \int d\omega \hbar\omega a_3^\dagger(\omega) a_3(\omega). \quad (6)$$

The linear coupling of the bath modes a_1 and a_2 to the cavity mode A is modeled by the hopping Hamiltonians

$$H_{T_1} = \hbar \int d\omega [\kappa_1 A^\dagger a_1(\omega) + \kappa_1^* a_1^\dagger(\omega) A] \quad (7)$$

and

$$H_{T_2} = \hbar \int d\omega [\kappa_2 A^\dagger a_2(\omega) + \kappa_2^* a_2^\dagger(\omega) A]. \quad (8)$$

The two-photon absorptive coupling of the resonator mode to the bath modes a_3 is modeled by a hopping Hamiltonian in which two cavity photons are destroyed for every bath photon created [19, 20, 21, 22, 23]

$$H_{T_3} = \hbar \int d\omega [\kappa_3 A^\dagger A^\dagger a_3(\omega) + \kappa_3^* a_3^\dagger(\omega) A A]. \quad (9)$$

All the modes in this model satisfy the usual boson commutation relations.

III. THE EQUATIONS OF MOTION

Since the creation and annihilation operators appearing in Eqs. (2) through (9) do not have an explicit time dependence, the Heisenberg equation of motion for these operators has the form

$$i\hbar \frac{dO}{dt} = [O, H] \quad (10)$$

where H is the total Hamiltonian. Using the boson commutation relation for the cavity mode

$$[A, A^\dagger] = A A^\dagger - A^\dagger A = 1, \quad (11)$$

one has

$$\begin{aligned} \frac{dA}{dt} &= -i\omega_0 A - iK A^\dagger A A \\ &- i\kappa_1 \int d\omega a_1(\omega) - i\kappa_2 \int d\omega a_2(\omega) - i2\kappa_3 \int d\omega A^\dagger a_3(\omega). \end{aligned} \quad (12)$$

Using the boson commutation relations for the bath modes

$$[a_i(\omega), a_j^\dagger(\omega')] = \delta_{i,j} \delta(\omega - \omega') \quad (13)$$

$$[a_i(\omega), a_j(\omega')] = 0, \quad (14)$$

one obtains the following equations for the bath modes $a_1(\omega)$, $a_2(\omega)$, and $a_3(\omega)$:

$$\frac{da_1(\omega)}{dt} = -i\omega a_1(\omega) - i\kappa_1^* A, \quad (15)$$

$$\frac{da_2(\omega)}{dt} = -i\omega a_2(\omega) - i\kappa_2^* A, \quad (16)$$

and

$$\frac{da_3(\omega)}{dt} = -i\omega a_3(\omega) - i\kappa_3^* A A. \quad (17)$$

Using the standard methods of Gardiner and Collett [15], these equations yield the following equation for the cavity mode A driven by the incoming bath modes a_i^{in} :

$$\begin{aligned} \frac{dA}{dt} &= -i\omega_0 A - iK A^\dagger A A - \gamma A - \gamma_3 A^\dagger A A \\ &- i\sqrt{2\gamma_1} e^{i\phi_1} a_1^{in}(t) - i\sqrt{2\gamma_2} e^{i\phi_2} a_2^{in}(t) \\ &- i2\sqrt{\gamma_3} e^{i\phi_3} A^\dagger a_3^{in}(t). \end{aligned} \quad (18)$$

where

$$\gamma = \gamma_1 + \gamma_2 \quad (19)$$

and the κ_i , which in general can be complex, have been reexpressed in terms of the positive real constants γ_i and the phases ϕ_i according to

$$\kappa_1 = \sqrt{\frac{\gamma_1}{\pi}} e^{i\phi_1}, \quad (20)$$

$$\kappa_2 = \sqrt{\frac{\gamma_2}{\pi}} e^{i\phi_2}, \quad (21)$$

$$\kappa_3 = \sqrt{\frac{\gamma_3}{2\pi}} e^{i\phi_3}. \quad (22)$$

In addition, the methods of Gardiner and Collett [15] yield the following relations between the outgoing bath modes a_i^{out} , the incoming bath modes a_i^{in} , and the cavity mode A :

$$a_1^{out}(t) - a_1^{in}(t) = -i\sqrt{2\gamma_1} e^{-i\phi_1} A(t), \quad (23)$$

$$a_2^{out}(t) - a_2^{in}(t) = -i\sqrt{2\gamma_2} e^{-i\phi_2} A(t), \quad (24)$$

$$a_3^{out}(t) - a_3^{in}(t) = -i\sqrt{2\gamma_3} e^{-i\phi_3} A(t) A(t). \quad (25)$$

In obtaining these equations a Markov approximation [15] has been made such that the boson annihilation operators $a_i^{in}(t)$ satisfy the commutation relations

$$[a_i^{in}(t), a_j^{in\dagger}(t')] = \delta_{i,j} \delta(t - t'), \quad (26)$$

$$[a_i^{in}(t), a_j^{in}(t')] = 0. \quad (27)$$

IV. RESPONSE TO A CLASSICAL PUMP

Operated as a negative-resistance reflection amplifier, an intense sinusoidal field, called the pump, is delivered to the input port of the device. Signals having frequencies to either side of the pump, but lying within the bandwidth of the device, will be amplified. The linearization procedure is now carried out in which the signals entering the input port and the noise entering the loss ports are considered to be small compared to the pump. The first step is to calculate the classical response of the device to an intense pump in the absence of signal and noise. The solution is then used to calculate the linearized response of the device in the presence of signal and noise.

In order to obtain the response of the device to a classical pump in the absence of signal and noise one sets the incoming noise terms to zero

$$a_2^{in} = 0, \quad (28)$$

$$a_3^{in} = 0. \quad (29)$$

The incoming pump is written as

$$a_1^{in} = b_1^{in} e^{-i(\omega_p t + \psi_1)} \quad (30)$$

where b_1^{in} is a real constant, ω_p is the pump frequency, and ψ_1 is the pump phase. The outgoing field will also have an oscillatory time dependence of frequency ω_p and can be written as

$$a_1^{out} = b_1^{out} e^{-i(\omega_p t + \psi_1)} \quad (31)$$

where b_1^{out} may be a complex constant. Writing A as

$$A = B e^{-i(\omega_p t + \phi_B)} \quad (32)$$

where B is a positive real constant, the equations of motion, Eqs. (18) and (23), yield

$$[i(\omega_0 - \omega_p) + \gamma]B + (iK + \gamma_3)B^3 = -i\sqrt{2\gamma_1} b_1^{in} e^{i(\phi_1 + \phi_B - \psi_1)} \quad (33)$$

and

$$b_1^{out} = b_1^{in} - i\sqrt{2\gamma_1} B e^{-i(\phi_1 + \phi_B - \psi_1)}. \quad (34)$$

Multiplying each side of the Eq. (33) by its complex conjugate and introducing

$$E = B^2, \quad (35)$$

one obtains

$$E^3 + \frac{2[(\omega_0 - \omega_p)K + \gamma\gamma_3]}{K^2 + \gamma_3^2} E^2 + \frac{(\omega_0 - \omega_p)^2 + \gamma^2}{K^2 + \gamma_3^2} E - \frac{2\gamma_1}{K^2 + \gamma_3^2} (b_1^{in})^2 = 0. \quad (36)$$

This cubic equation will have one real solution and two complex solutions or three real solutions. For the case when two of the solutions are complex, the real solution is the physical solution. If there are three solutions, two will be stable and one unstable, and the device will exhibit bistability. Once E and, hence, B have been determined from Eqs. (36) and (35), the phase ϕ_B can be determined from Eq. (33) and the amplitude of the reflected pump can then be computed from Eq. (34). In Fig. 2 (a), (d), and (g) plots of B as a function of frequency for three different incoming pump amplitudes are shown. The frequency pulling of the cavity resonance is clearly seen in (d) and (g) as the incoming pump amplitude b_1^{in} is increased. Also plotted in Fig. 2 (b), (e), and (g) is the reflection coefficient $|b_1^{out}/b_1^{in}|$ for the reflected pump amplitude as a function of frequency. If no power were absorbed by the cavity, the reflection coefficient would be unity. One sees a dip in the reflected power at the cavity resonance. As the incoming pump amplitude is increased, this absorption feature also shows frequency pulling, as can be seen in (e) and (g).

A. Special operating points

As a function of the pump frequency ω_p , B will have the form of the distorted Lorentzian curve (see Fig. 2

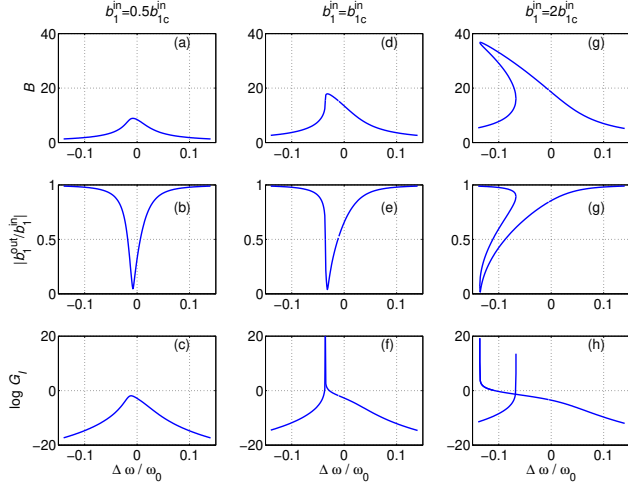


FIG. 2: The cavity-mode amplitude $|B|$, the reflection amplitude $|b_1^{in}/b_1^{out}|$, and the intermodulation gain G_I for vanishing offset frequency $\omega = 0$ shown for sub-critical case $b_1^{in} = 0.5b_1^{in_c}$, critical case $b_1^{in} = b_1^{in_c}$, and above-critical case $b_1^{in} = 2b_1^{in_c}$. In all cases $K = -10^{-4}\omega_0$, $\gamma_1 = 0.01\omega_0$, $\gamma_2 = 1.1\gamma_1$, and $\gamma_3 = 0.01K/\sqrt{3}$. For $b_1^{in} > b_1^{in_c}$ the response becomes multi-value function of frequency in some frequency range.

(a), (d), and (g)) exhibited by Duffing oscillators [24, 25, 26]. The maximum of the response curve occurs when $\partial E/\partial\omega_p = 0$. This condition yields

$$\omega_0 - \omega_p + KE = 0, \quad (37)$$

that is, the peak of the resonance curve is shifted by an amount KB^2 . The points of instability where the system will switch from one of the two bistable states to the other are located where $\partial\omega_p/\partial E = 0$. This condition is satisfied when

$$(\gamma + 2\gamma_3 E)^2 = (K^2 + \gamma_3^2)E^2 - (\omega_0 - \omega_p + 2KE)^2. \quad (38)$$

When, in addition, $\partial^2\omega_p/\partial E^2 = 0$, the two points of instability coalesce into a single point. The condition $\partial^2\omega_p/\partial E^2 = 0$ is satisfied when

$$6(K^2 + \gamma_3^2)E + 4[(\omega_0 - \omega_p)K + \gamma\gamma_3] = 0. \quad (39)$$

Large parametric gain is achieved at points where the slope of E with respect to ω_p becomes infinite, but in order to remain stable it is desirable to operate the reflection parametric amplifier near the critical point with parameters chosen so that the Duffing curve does not have a bistable region. It is a straightforward exercise to show that in order for the resonance curve to have a critical point at which both Eqs. (38) and (39) are satisfied, one must have

$$|K| > \sqrt{3}\gamma_3. \quad (40)$$

At the critical point one has

$$E_c = \frac{2\gamma}{\sqrt{3}(|K| - \sqrt{3}\gamma_3)} \quad (41)$$

and

$$\omega_0 - \omega_p = -\gamma \frac{K}{|K|} \left[\frac{4\gamma_3|K| + \sqrt{3}(K^2 + \gamma_3^2)}{K^2 - 3\gamma_3^2} \right]. \quad (42)$$

The incoming pump amplitude required for operation at the critical point is given by

$$(b_{1c}^{in})^2 = \frac{4}{3\sqrt{3}} \frac{\gamma^3(K^2 + \gamma_3^2)}{\gamma_1(|K| - \sqrt{3}\gamma_3)^3}. \quad (43)$$

When $\gamma_3 = 0$ these reduce to

$$E_c = \frac{2\sqrt{3}\gamma}{3|K|}, \quad (44)$$

$$\omega_0 - \omega_p = -\sqrt{3}\gamma \frac{K}{|K|}, \quad (45)$$

$$(b_{1c}^{in})^2 = \frac{4}{3\sqrt{3}} \frac{\gamma^3}{\gamma_1|K|}. \quad (46)$$

In panel (d) of Fig. 2 the amplitude of the cavity mode as a function of frequency has been plotted for the case when the incoming pump amplitude is that of the critical pump amplitude. One sees that the line shape of the cavity mode is vertical at a point on the lower side of the resonance. The line shape of the reflected power is shown in panel (e) of Fig. 2.

V. LINEARIZATION

A linearized analysis is now performed in which the incoming signal and the noise from the losses are regarded as small compared to the pump. To that end we write

$$a_1^{in} = b_1^{in} e^{-i(\omega_p t + \psi_1)} + c_1^{in} e^{-i\omega_p t}, \quad (47)$$

$$a_2^{in} = c_2^{in} e^{-i\omega_p t}, \quad (48)$$

$$a_3^{in} = c_3^{in} e^{-i\omega_p t}, \quad (49)$$

$$a_1^{out} = b_1^{out} e^{-i(\omega_p t + \psi_1)} + c_1^{out} e^{-i\omega_p t}, \quad (50)$$

$$a_2^{out} = b_2^{out} e^{-i\omega_p t} + c_2^{out} e^{-i\omega_p t}, \quad (51)$$

$$a_3^{out} = b_3^{out} e^{-i\omega_p t} + c_3^{out} e^{-i\omega_p t}, \quad (52)$$

and

$$A = B e^{-i(\omega_p t + \phi_B)} + a e^{-i\omega_p t} \quad (53)$$

where B , b_1^{out} , b_2^{out} and b_3^{out} constitute the solution for the response of the system to a classical pump in the absence of signal and noise. The properties of this solution have already been discussed in Section 4. The c_1^{in} , c_2^{in} , c_3^{in} , c_1^{out} , c_2^{out} , c_3^{out} , and a are regarded as small and will be kept only up to linear order. Substituting these into the equations of motion yields

$$\begin{aligned} \frac{da}{dt} = & -[i(\omega_0 - \omega_p) + \gamma]a - 2(iK + \gamma_3)B^2a \\ & - (iK + \gamma_3)B^2e^{-i2\phi_B}a^\dagger - i\sqrt{2\gamma_1}e^{i\phi_1}c_1^{in} \\ & - i\sqrt{2\gamma_2}e^{i\phi_2}c_2^{in} - i2\sqrt{\gamma_3}Be^{i(\omega_p t + \phi_B + \phi_3)}c_3^{in}, \end{aligned} \quad (54)$$

$$c_1^{out} - c_1^{in} = -i\sqrt{2\gamma_1}e^{-i\phi_1}a, \quad (55)$$

$$c_2^{out} - c_2^{in} = -i\sqrt{2\gamma_2}e^{-i\phi_2}a, \quad (56)$$

$$c_3^{out} - c_3^{in} = -i2\sqrt{\gamma_3}Be^{-i(\omega_p t + \phi_B + \phi_3)}a. \quad (57)$$

VI. SOLVING THE LINEARIZED EQUATION

Introducing

$$W = i(\omega_0 - \omega_p) + \gamma + 2(iK + \gamma_3)B^2, \quad (58)$$

$$V = (iK + \gamma_3)B^2e^{-2i\phi_B}, \quad (59)$$

and

$$\begin{aligned} F = & -i\sqrt{2\gamma_1}e^{i\phi_1}c_1^{in} - i\sqrt{2\gamma_2}e^{i\phi_2}c_2^{in} \\ & - i2\sqrt{\gamma_3}Be^{i(\omega_p t + \phi_B + \phi_3)}c_3^{in}, \end{aligned} \quad (60)$$

the linearized equation of motion can be written in the form

$$\frac{da}{dt} + Wa + Va^\dagger = F. \quad (61)$$

From this last equation one obtains

$$\frac{d^2a}{dt^2} + 2\Re(W)\frac{da}{dt} + (|W|^2 - |V|^2)a = \Gamma(t) \quad (62)$$

where

$$\Gamma(t) = \frac{dF}{dt} + W^*F - VF^\dagger(t). \quad (63)$$

Writing

$$a = e^{-\lambda t}, \quad (64)$$

the characteristic equation for the homogenous equation is given by

$$\lambda^2 - 2\Re(\omega)\lambda + |W|^2 - |V|^2 = 0. \quad (65)$$

This has the two roots

$$\lambda_0 = \Re(W) - \sqrt{\Re^2(W) - |W|^2 + |V|^2}, \quad (66)$$

$$\lambda_1 = \Re(W) + \sqrt{\Re^2(W) - |W|^2 + |V|^2}, \quad (67)$$

or

$$\lambda_0 = \gamma + 2\gamma_3B^2 - \sqrt{(K^2 + \gamma_3^2)B^4 - (\omega_0 - \omega_p + 2KB^2)^2}, \quad (68)$$

$$\lambda_1 = \gamma + 2\gamma_3B^2 + \sqrt{(K^2 + \gamma_3^2)B^4 - (\omega_0 - \omega_p + 2KB^2)^2}. \quad (69)$$

The root λ_0 is zero when Eq. (38) is satisfied, that is, one has critical slowing down at the points where the slope of E with respect to ω_p is infinite.

Introducing the Fourier transforms

$$a(t) = \frac{1}{\sqrt{2\pi}} \int_{-\infty}^{\infty} d\omega a(\omega)e^{-i\omega t}, \quad (70)$$

$$c_1(t) = \frac{1}{\sqrt{2\pi}} \int_{-\infty}^{\infty} d\omega c_1(\omega)e^{-i\omega t}, \quad (71)$$

$$c_2(t) = \frac{1}{\sqrt{2\pi}} \int_{-\infty}^{\infty} d\omega c_2(\omega)e^{-i\omega t}, \quad (72)$$

$$c_3(t) = \frac{1}{\sqrt{2\pi}} \int_{-\infty}^{\infty} d\omega c_3(\omega)e^{-i\omega t}, \quad (73)$$

$$\Gamma(t) = \frac{1}{\sqrt{2\pi}} \int_{-\infty}^{\infty} d\omega \Gamma(\omega)e^{-i\omega t}, \quad (74)$$

Eq. (62) yields

$$a(\omega) = \frac{\Gamma(\omega)}{-\omega^2 - 2i\omega\Re(W) + (|W|^2 - |V|^2)}. \quad (75)$$

In terms of the roots of the characteristic equation this can be written as

$$a(\omega) = \frac{\Gamma(\omega)}{(-i\omega + \lambda_0)(-i\omega + \lambda_1)} \quad (76)$$

where

$$\begin{aligned} \Gamma(\omega) = & -i\sqrt{2\gamma_1}[(-i\omega + W^*)e^{i\phi_1}c_1^{in}(\omega) - V e^{-i\phi_1}c_1^{in\dagger}(-\omega)] \\ & - i\sqrt{2\gamma_2}[(-i\omega + W^*)e^{i\phi_2}c_2^{in}(\omega) - V e^{-i\phi_2}c_2^{in\dagger}(-\omega)] \\ & - i2\sqrt{\gamma_3}B[(-i\omega + W^*)e^{i(\phi_B + \phi_3)}c_3^{in}(\omega_p + \omega) \\ & - V e^{-i(\phi_B + \phi_3)}c_3^{in\dagger}(\omega_p - \omega)]. \end{aligned} \quad (77)$$

A. The output field

From Eq. (23) one obtains

$$c_1^{out}(\omega) = c_1^{in}(\omega) - i\sqrt{2\gamma_1}e^{-i\phi_1}a(\omega). \quad (78)$$

Substituting Eq. (76) into this equation yields

$$\begin{aligned} c_1^{out}(\omega) \\ = \frac{(-i\omega + \lambda_0)(-i\omega + \lambda_1)c_1^{in}(\omega) - i\sqrt{2\gamma_1}e^{-i\phi_1}\Gamma(\omega)}{(-i\omega + \lambda_0)(-i\omega + \lambda_1)} \end{aligned} \quad (79)$$

or

$$\begin{aligned} c_1^{out}(\omega) \\ = \frac{(-i\omega + \lambda_0)(-i\omega + \lambda_1) - 2\gamma_1(-i\omega + W^*)}{(-i\omega + \lambda_0)(-i\omega + \lambda_1)}c_1^{in}(\omega) \\ + \frac{2\gamma_1 V e^{-i2\phi_1}}{(-i\omega + \lambda_0)(-i\omega + \lambda_1)}c_1^{in\dagger}(-\omega) \\ - \frac{2\sqrt{\gamma_1\gamma_2}(-i\omega + W^*)e^{-i(\phi_1 - \phi_2)}}{(-i\omega + \lambda_0)(-i\omega + \lambda_1)}c_2^{in}(\omega) \\ + \frac{2\sqrt{\gamma_1\gamma_2}V e^{-i(\phi_1 + \phi_2)}}{(-i\omega + \lambda_0)(-i\omega + \lambda_1)}c_2^{in\dagger}(-\omega) \\ - \frac{2\sqrt{2\gamma_1\gamma_3}B(-i\omega + W^*)e^{-i(\phi_1 - \phi_B - \phi_3)}}{(-i\omega + \lambda_0)(-i\omega + \lambda_1)}c_3^{in}(\omega_p + \omega) \\ + \frac{2\sqrt{2\gamma_1\gamma_3}B V e^{-i(\phi_1 + \phi_3 + \phi_B)}}{(-i\omega + \lambda_0)(-i\omega + \lambda_1)}c_3^{in\dagger}(\omega_p - \omega). \end{aligned} \quad (80)$$

The linearized solution to the equations of motion has now been obtained. We will now evaluate the properties of this solution for various kinds of inputs.

VII. PARAMETRIC AND INTERMODULATION GAIN

The parametric gain and the intermodulation gain are calculated by taking $c_1^{in}(\omega)$ to represent a classical signal at frequency $\omega_p + \omega$. Setting all other signal and noise inputs to zero, Eq. (80) yields the following power gain for the reflected signal:

$$\begin{aligned} G_S &\equiv \frac{|c_1^{out}(\omega)|^2}{|c_1^{in}(\omega)|^2} \\ &= \frac{|(-i\omega + \lambda_0)(-i\omega + \lambda_1) - 2\gamma_1(-i\omega + W^*)|^2}{(\omega^2 + \lambda_0^2)(\omega^2 + \lambda_1^2)}. \end{aligned} \quad (81)$$

When this quantity becomes greater than unity one has parametric amplification of the signal.

As seen from Eq. (80), a signal $c_{in}(-\omega)$ injected at frequency $\omega_p - \omega$ will generate an output signal at frequency $\omega_p + \omega$. This frequency conversion is quantified by

the intermodulation conversion gain defined by

$$\begin{aligned} G_I &\equiv \frac{|c_1^{out}(\omega)|^2}{|c_1^{in}(-\omega)|^2} \\ &= \frac{4\gamma_1^2|V|^2}{(\omega^2 + \lambda_0^2)(\omega^2 + \lambda_1^2)}. \end{aligned} \quad (82)$$

Since the output signal at $\omega_p + \omega$ is separated in frequency from the input signal, the measurement of the intermodulation gain is a particularly sensitive method for measuring the strength of the nonlinearities. We note that, even without power gain, devices capable of producing intermodulation signals are useful as mixers. When $\omega = 0$, both the expression for G_S and the expression for G_I will have $\lambda_0^2\lambda_1^2$ in the denominator. As one approaches an operating point where the slope of E with respect to ω_p becomes infinite, both the parametric gain and the intermodulation conversion gain will diverge. Hence, it is near the instability points where the device can exhibit large gains. Panels (c), (f), and (h) of Fig. 2 show the behavior of the intermodulation gain as the pump amplitude is increased from half critical (c) to critical (f) to twice critical (h) as a function of frequency. As depicted in panel (f) at the critical point the intermodulation gain diverges. Above critical, as shown in panel (h), the intermodulation gain diverges as one approaches the points of infinite slope on the resonance curve (g).

VIII. NOISE SQUEEZING

Because of intermodulation gain, a parametric amplifier can establish correlations [27] between the output at $\omega_p + \omega$ and $\omega_p - \omega$. When delivered to a mixer whose local oscillator is phase-locked to the pump these correlations can result in noise fluctuations reduced below that which the mixer would see if the signal delivered to the parametric amplifier were, instead, directly delivered to the mixer. This noise reduction is called squeezing, and it can occur with either thermal or quantum noise [5]. We now obtain expressions that will allow one to calculate the degree of thermal or quantum noise squeezing. For such a calculation the c_1^{in} , c_2^{in} , c_3^{in} , c_1^{out} , c_2^{out} , c_3^{out} are again treated as quantum mechanical operators satisfying commutation relations of the form Eqs. (26) and (27).

The output of a mixer, operated in the homodyne mode in which the local oscillator frequency ω_{LO} and the pump frequency ω_p are equal and in which the input at the signal frequency $\omega_{LO} + \omega$ and at the image frequency $\omega_{LO} - \omega$ are both regarded as signal, is given by [4]

$$I_D(\omega) = c_1^{out\dagger}(-\omega)e^{-i\phi_{LO}} + c_1^{out}(\omega)e^{i\phi_{LO}} \quad (83)$$

where ϕ_{LO} is the local oscillator phase. To evaluate the mean value and the power spectrum for the homodyne

detector output it is necessary to specify the density matrix for the signal and noise entering the parametric amplifier. Here we consider the case when these inputs consist of Nyquist noise. In this case one has

$$\langle c_i^{in}(\omega) \rangle = 0 , \quad (84)$$

$$\langle c_i^{in\dagger}(\omega) c_j^{in}(\omega') \rangle = \frac{e^{-\beta_i \hbar \omega_p}}{1 - e^{-\beta_i \hbar \omega_p}} \delta_{i,j} \delta(\omega - \omega') , \quad (85)$$

and

$$\langle c_i^{in}(\omega) c_j^{in}(\omega') \rangle = 0 . \quad (86)$$

Here

$$\beta_i = \frac{1}{k_B T_i} , \quad (87)$$

where k_B is Boltzmann's constant and T_i is the absolute temperature of the bath for which $c_i^{in}(\omega)$ is the incoming mode. We thus allow each of the baths to be at a different temperature. In writing Eq. (85) we have made the approximation that the frequencies ω of interest are small compared to ω_p .

Because Eq. (80) is linear in the $c_i^{in}(\omega)$ it is evident that

$$\langle I_D(\omega) \rangle = 0 , \quad (88)$$

that is, the homodyne detector output consists of noise fluctuations with zero mean. Because of the boson commutation relations, one has

$$\langle I_D^\dagger(\omega) I_D(\omega') \rangle = P(\omega) \delta(\omega - \omega') \quad (89)$$

where $P(\omega)$ is the noise power spectrum of the homodyne detector output. Equation (80) can be rewritten as

$$\begin{aligned} c_1^{out}(\omega) &= A_1(\omega) c_1^{in}(\omega) + B_1(\omega) c_1^{in\dagger}(-\omega) \\ &+ A_2(\omega) c_2^{in}(\omega) + B_2(\omega) c_2^{in\dagger}(-\omega) \\ &+ A_3(\omega) c_3^{in}(\omega_p + \omega) + B_3(\omega) c_3^{in\dagger}(\omega_p - \omega) \end{aligned} \quad (90)$$

where

$$A_1(\omega) = \frac{(-i\omega + \lambda_0)(-i\omega + \lambda_1) - 2\gamma_1(-i\omega + W^*)}{(-i\omega + \lambda_0)(-i\omega + \lambda_1)} , \quad (91)$$

$$B_1(\omega) = \frac{2\gamma_1 V e^{-i2\phi_1}}{(-i\omega + \lambda_0)(-i\omega + \lambda_1)} , \quad (92)$$

$$A_2(\omega) = -\frac{2\sqrt{\gamma_1 \gamma_2}(-i\omega + W^*) e^{-i(\phi_1 - \phi_2)}}{(-i\omega + \lambda_0)(-i\omega + \lambda_1)} , \quad (93)$$

$$B_2(\omega) = \frac{2\sqrt{\gamma_1 \gamma_2} V e^{-i(\phi_1 + \phi_2)}}{(-i\omega + \lambda_0)(-i\omega + \lambda_1)} , \quad (94)$$

$$A_3(\omega) = -\frac{2\sqrt{2\gamma_1 \gamma_3} B(-i\omega + W^*) e^{-i(\phi_1 - \phi_B - \phi_3)}}{(-i\omega + \lambda_0)(-i\omega + \lambda_1)} , \quad (95)$$

$$B_3(\omega) = \frac{2\sqrt{2\gamma_1 \gamma_3} B V e^{-i(\phi_1 + \phi_3 + \phi_B)}}{(-i\omega + \lambda_0)(-i\omega + \lambda_1)} . \quad (96)$$

Substituting Eq. (90) into Eq. (83), evaluating $\langle I_D^\dagger(\omega) I_D(\omega') \rangle$ using Eq. (85), and then reading off the power spectrum using Eq. (89), one obtains

$$\begin{aligned} P(\omega) &= |e^{-i\phi_{LO}} A_1^*(\omega) + e^{i\phi_{LO}} B_1(-\omega)|^2 \frac{e^{-\beta_1 \hbar \omega_p}}{1 - e^{-\beta_1 \hbar \omega_p}} \\ &+ |e^{i\phi_{LO}} A_1(-\omega) + e^{-i\phi_{LO}} B_1^*(\omega)|^2 \frac{1}{1 - e^{-\beta_1 \hbar \omega_p}} \\ &+ |e^{-i\phi_{LO}} A_2^*(\omega) + e^{i\phi_{LO}} B_2(-\omega)|^2 \frac{e^{-\beta_2 \hbar \omega_p}}{1 - e^{-\beta_2 \hbar \omega_p}} \\ &+ |e^{i\phi_{LO}} A_2(-\omega) + e^{-i\phi_{LO}} B_2^*(\omega)|^2 \frac{1}{1 - e^{-\beta_2 \hbar \omega_p}} \\ &+ |e^{-i\phi_{LO}} A_3^*(\omega) + e^{i\phi_{LO}} B_3(-\omega)|^2 \frac{e^{-\beta_3 \hbar \omega_p}}{1 - e^{-\beta_3 \hbar \omega_p}} \\ &+ |e^{i\phi_{LO}} A_3(-\omega) + e^{-i\phi_{LO}} B_3^*(\omega)|^2 \frac{1}{1 - e^{-\beta_3 \hbar \omega_p}} . \end{aligned} \quad (97)$$

This formula may be used to compute the noise-power spectrum for any local oscillator phase ϕ_{LO} and any set of device parameters. It is useful to consider the case when there is no incoming pump field and the input field and loss baths are all at zero temperature. In this case the field reflected off the input port of the amplifier will consist of vacuum fluctuations, that is,

$$c_1^{out}(\omega) |0\rangle = 0 , \quad (98)$$

and one obtains

$$\langle I_D^\dagger(\omega) I_D(\omega') \rangle = \delta(\omega - \omega') \quad (99)$$

or

$$P(\omega) = 1 . \quad (100)$$

This sets the vacuum noise level for the conventions we are using. As is shown in Fig. 3 and as will be illustrated with specific examples in the next section, under suitable circumstances it is possible to obtain reflected signals whose noise-power spectrum $P(\omega)$, for certain local oscillator phase settings, is less than 1. Such signals are said to be squeezed below the vacuum noise level. Figure 3 shows the minimum value of $P(\omega)$ as a function of the amplitude of the incoming pump b_1^{in} when the bath temperatures are all zero, the strength of the Kerr nonlinearity is chosen to be $K = 5\omega_0$, and the coupling strength of the signal to the cavity mode is taken to be $\gamma_1 = 0.0001\omega_0$. The pump frequency has been chosen to be that of the critical pump frequency. The solid line is the lossless case when $\gamma_2 = \gamma_3 = 0$. In this case complete

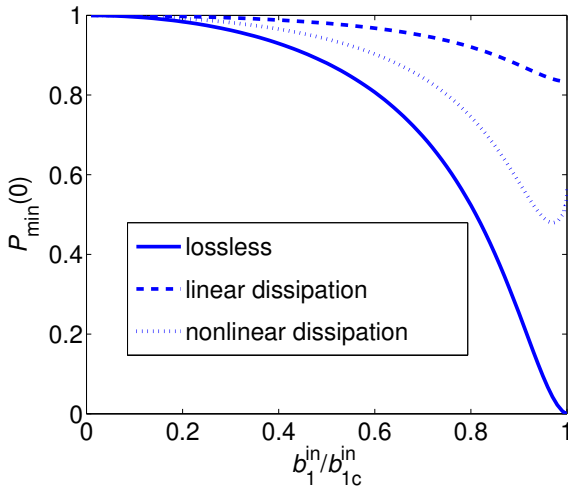


FIG. 3: Examples of achievable degree of squeezing, $P_{min}(0)$ vs. b_1^{in}/b_{1c}^{in} . In all plots $T_1 = T_2 = T_3 = 0$, $K = 5\omega_0$, $\gamma_1 = 0.0001\omega_0$, and the pump frequency ω_p obtains its critical value, as given by Eq. 42. The solid line represents the lossless case, where $\gamma_2 = \gamma_3 = 0$. The dashed line represents the case of linear dissipation where $\gamma_2 = 5\gamma_1$ and $\gamma_3 = 0$, while the dotted line represents the case of nonlinear dissipation where $\gamma_2 = 0$ and $\gamma_3 = 0.5K/\sqrt{3}$.

squeezing $P(0) = 0$ is possible when the incoming pump power is at the critical value, that is, $|b_1^{in}/b_{1c}^{in}| = 1$. The dashed curve represents the case when the linear dissipation is given by $\gamma_2 = 5\gamma_1$ and the nonlinear dissipation γ_3 is zero. In general, the presence of linear dissipation reduces the amount of achievable squeezing. The dotted line depicts the case when the linear dissipation is zero and the nonlinear dissipation is given by $\gamma_3 = 0.5K/\sqrt{3}$. Nonlinear dissipation also tends to reduce the amount of squeezing that can be produced. However, nonlinear dissipation can produce some squeezing in the absence of a Kerr medium, as we discuss below.

A. Special cases

It is instructive to evaluate Eq. (97) for a few specific cases. In particular, the power spectrum at $\omega = 0$ reduces to

$$\begin{aligned} P(0) &= |e^{-i\phi_{LO}} A_1^*(0) + e^{i\phi_{LO}} B_1(0)|^2 \coth\left(\frac{\hbar\omega_p}{2k_B T_1}\right) \\ &+ |e^{-i\phi_{LO}} A_2^*(0) + e^{i\phi_{LO}} B_2(0)|^2 \coth\left(\frac{\hbar\omega_p}{2k_B T_2}\right) \\ &+ |e^{-i\phi_{LO}} A_3^*(0) + e^{i\phi_{LO}} B_3(0)|^2 \coth\left(\frac{\hbar\omega_p}{2k_B T_3}\right). \end{aligned} \quad (101)$$

Further simplification results from considering the case when the internal losses are all zero. In this case $\gamma_2 = 0$

and $\gamma_3 = 0$. Thus, the terms in Eq. (101) corresponding to internally generated noise vanish and one obtains

$$P(0) = |e^{-i\phi_{LO}} A_1^*(0) + e^{i\phi_{LO}} B_1(0)|^2 \coth\left(\frac{\hbar\omega_p}{2k_B T_1}\right). \quad (102)$$

Writing

$$A_1(0) = |A_1(0)|e^{i\phi_A}, \quad (103)$$

$$B_1(0) = |B_1(0)|e^{i\phi_B}, \quad (104)$$

one has

$$P(0) = |A_1(0)| + |B_1(0)|e^{i\psi}|^2 \coth\left(\frac{\hbar\omega_p}{2k_B T_1}\right) \quad (105)$$

where

$$\psi = 2\phi_{LO} - \phi_A + \phi_B. \quad (106)$$

$P(0)$ is maximized when the local oscillator phase ϕ_{LO} is chosen so that

$$e^{i\psi} = 1. \quad (107)$$

In this case one obtains

$$P_{max}(0) = (|A_1(0)| + |B_1(0)|)^2 \coth\left(\frac{\hbar\omega_p}{2k_B T_1}\right). \quad (108)$$

$P(0)$ is minimized when the local oscillator phase ϕ_{LO} is chosen so that

$$e^{i\psi} = -1. \quad (109)$$

In this case one obtains

$$P_{min}(0) = (|A_1(0)| - |B_1(0)|)^2 \coth\left(\frac{\hbar\omega_p}{2k_B T_1}\right). \quad (110)$$

From Eqs. (106), (107), and (109) it follows that the local oscillator phase at which the spectral density $P(0)$ is minimized differs by $\pi/2$ from the local oscillator phase at which the spectral density is maximized, that is, the signal components minimizing and maximizing the spectral density are in quadrature. It is straightforward to show that

$$|A_1(0)|^2 - |B_1(0)|^2 = 1. \quad (111)$$

From this equation and Eqs. (108) and (110), one obtains

$$P_{max}(0)P_{min}(0) = \coth^2\left(\frac{\hbar\omega_p}{2k_B T_1}\right). \quad (112)$$

Hence, in the case of no loss, the degree of amplification and the degree of deamplification of the noise are the same. For this case one also has

$$|B_1(0)| = \frac{2\gamma_1 K B^2}{(\omega_0 - \omega_p + 2KB^2)^2 + \gamma_1^2 - K^2 B^4}. \quad (113)$$

Note that $|B_1(0)|$ can be made arbitrarily large by choosing the pump frequency ω_p and the pump amplitude B such that the denominator goes to zero. From this it follows that P_{max} can be made arbitrarily large and P_{min} can be made arbitrarily small. In practice, higher order terms responsible for pump depletion will limit how big P_{max} can be made.

Noise from the losses and gain saturation will limit the maximum degree of noise squeezing to be below that calculated here. This is demonstrated in Figure 3, where the achievable degree of squeezing $P_{min}(0)$ is plotted as a function of b_1^{in}/b_{1c}^{in} for some examples in which the linear or nonlinear loss is taken to be nonzero.

The presence of a two-photon loss allows for squeezing even in the absence of a Kerr nonlinearity [22]. Setting $K = 0$, $\gamma_2 = 0$, and $\omega_0 = \omega_p$, the greatest degree of squeezing of the output field of the cavity occurs when $\gamma_1 = 3\gamma_3 B^2$. At this operating point $P(0) = 2/3$ and the local oscillator phase must be adjusted so that $\cos(2\phi_{LO} - 2\phi_B - 2\phi_1) = 1$.

IX. CONCLUSIONS

We have presented an analysis of a cavity parametric amplifier employing a Kerr nonlinearity but which also possesses a two-photon loss. We have obtained expressions for the pump amplitude inside the cavity and the reflected pump amplitude for the case when pump saturation can be neglected. We have obtained expressions for the classical gain and the intermodulation gain. These expressions are useful for determining model parameters from experimental data. We have also obtained expressions from which one can compute the degree of squeezing that the device exhibits. Both the linear and nonlinear loss tend to degrade the amount of squeezing that can be achieved, although even without a Kerr nonlinearity a modest amount of squeezing can be achieved by the two-photon loss.

[1] J. R. Tucker, IEEE J. Quantum Electron. **QE-15**, 1234 (1979).

[2] J. R. Tucker and M. J. Feldman, Rev. Mod. Phys. **57**, 1055 (1985).

[3] L. S. Kuzmin, K. K. Likharev, V. V. Migulin, and A. B. Zorin, IEEE Trans. Magn. **MAG-19**, 618 (1983).

[4] B. Yurke, L. R. Corruccini, P. G. Kaminsky, L. W. Rupp, A. D. Smith, A. H. Silver, R. W. Simon, and E. A. Whitaker, Phys. Rev. A, **39**, 2519 (1989).

[5] R. Movshovich, B. Yurke, P. G. Kaminsky, A. D. Smith, A. H. Silver, R. W. Simon, and M. V. Schneider, Phys. Rev. Lett. **65**, 1419 (1990).

[6] T. Dahm and D. J. Scalapino, J. App. Phys. **81**, 2002 (1997).

[7] B. Abdo, E. Segev, O. Shtempluck, and E. Buks, arXiv:cond-mat/0501114v2 10 Jan 2005, arXiv:cond-mat/0504582 22 April 2005.

[8] A. Villeneuve, C. C. Yang, G. I. Stegeman, C-H. Lin, and H-H Lin, Appl. Phys. Lett. **62**, 2465 (1993).

[9] A. M. Fox, J. J. Baumberg, M. Dabbiacco, B. Huttner, and J. F. Ryan, Phys. Rev. Lett. **74**, 1728 (1995).

[10] S-T. Ho, X. Zhang, and M. K. Udo, J. Opt. Soc. Am. B **12**, 1537 (1995).

[11] S. Zaitsev and E. Buks, arXiv:cond-mat/053130v1 6 Mar 2005.

[12] C. C. Gerrry and E. E. Hach III, Opt. Commun. **100**, 211 (1993).

[13] L. Gilles, B. M. Garraway, and P. L. Knight, Phys. Rev. A **49**, 2785 (1994).

[14] GX. Li, JS. Peng, and P. Zhou, Chinese Physics Letters **12**, 79 (1995).

[15] C. W. Gardiner and M. J. Collett, Phys. Rev. A **31**, 3761 (1985).

[16] J. Gea-Banacloche, N. Lu, L. M. Pedrotti, S. Prasad, M. O. Scully, and K. Wodkiewich, Phys. Rev. A **41**, 369 (1990).

[17] N. Imoto, H. A. Haus, and Y. Yamamoto, Phys. Rev. A **32**, 2287 (1985).

[18] A. G. White, P. K. Lam, D. E. McClelland, H-A. Bachor, and J. Munro, J. Opt. B **2**, 553 (2000).

[19] N. Tornau and A. Bach, Opt. Commun. **11**, 46 (1974).

[20] G. S. Agarwal and G. P. Hildred, Opt. Comm. **58**, 287 (1986).

[21] L. Gilles and P. L. Knight, Phys. Rev. A **48**, 1582 (1993).

[22] H. Ezaki, J. Phys. Soc. Japan, **68**, 1562 (1999).

[23] M. Kitamura and T. Tokihiro, J. Opt. B **1**, 546 (1999).

[24] A. H. Nayfeh and D. T. Mook, *Nonlinear Oscillations*, (Wiley, 1979).

[25] L. D. Landau, *Mechanics*, 3rd Ed., (Pergamon, 1976).

[26] B. Yurke, D. S. Greywall, A. N. Pargellis, and P. A. Busch, Phys. Rev. A **51**, 4211 (1995).

[27] B. Yurke, Phys. Rev. A, **32**, 300 (1985).